NASA TECHNICAL NOTE

NASA TN D-7058

NASA TN D-7058

PISTON MANOMETER AS AN ABSOLUTE STANDARD FOR VACUUM-GAGE CALIBRATION IN THE RANGE 10 TO 700 MICROTORR

by Isidore Warshawsky

Lewis Research Center
Cleveland, Ohio 44135

NATIONAL AERONAUTICS AND SPACE ADMINISTRATION • WASHINGTON, D. C. • NOVEMBER 1972

1. Report No.	2. Government Accession No.	3. Recipient's Catalog No.
NASA TN D-7058		

4. Title and Subtitle	5. Report Date
PISTON MANOMETER AS AN ABSOLUTE STANDARD FOR VACUUM-GAGE CALIBRATION IN THE RANGE 10 TO 700 MICROTORR	November 1972
	6. Performing Organization Code
7. Author(s) Isidore Warshawsky	8. Performing Organization Report No. E-6971
	10. Work Unit No. 502-04
9. Performing Organization Name and Address Lewis Research Center National Aeronautics and Space Administration Cleveland, Ohio 44135	11. Contract or Grant No.
	13. Type of Report and Period Covered Technical Note
12. Sponsoring Agency Name and Address National Aeronautics and Space Administration Washington, D.C. 20546	14. Sponsoring Agency Code

15. Supplementary Notes

16. Abstract

Total pressure in a calibration chamber is determined by measuring the force on a disk suspended in an orifice in the baseplate of the chamber. The disk forms a narrow annular gap with the orifice. A continuous flow of calibration gas passes through the chamber and annulus to a downstream pumping system. The ratio of pressures on the two faces of the disk exceeds 100:1, so that chamber pressure is substantially equal to the product of disk area and net force on the disk. This force is measured with an electrodynamometer that can be calibrated in situ with dead weights. Probable error in pressure measurement is ±(0.5 microtorr + 0.6 percent).

17. Key Words (Suggested by Author(s))

Calibration
Manometer, piston
Measurement, vacuum
Pressure measurement
Vacuum gages
Standards

18. Distribution Statement

Unclassified - unlimited

19. Security Classif. (of this report)	20. Security Classif. (of this page)	21. No. of Pages	22. Price*
Unclassified	Unclassified	39	$3.00

* For sale by the National Technical Information Service, Springfield, Virginia 22151

CONTENTS

PISTON MANOMETER AS AN ABSOLUTE STANDARD FOR VACUUM-GAGE CALIBRATION IN THE RANGE 10 TO 700 MICROTORR

by Isidore Warshawsky

Lewis Research Center

SUMMARY

Total pressure in a calibration chamber is determined by measuring the force on a flat, cylindrical piston suspended in a knife-edged orifice in the bottom, horizontal wall of the chamber. The piston is about 100 square centimeters in area and almost fills the orifice, leaving an annular gap of about 0.2 millimeter. A continuous flow of calibration gas, injected into the chamber through a leak valve to maintain the desired pressure, passes through the annular gap to a diffusion pump. The ratio of pressures on the two faces of the piston exceeds 100:1 so that downstream pressure need be known only nominally to deduce upstream pressure. The measurement depends principally on area and force measurements. The force-measuring device is calibrated with dead weights. Probable error in total-pressure measurement is ±(0.5 microtorr + 0.6 percent). Probable error in measuring the net pressure of the calibrating gas depends on the extent to which contaminating gases are present; it is estimated to be ±(0.7 microtorr + 0.6 percent) for inert-gas pressures above 10 microtorr and not to exceed ±(1 microtorr + 1 percent) for gases as active as water or hydrogen.

INTRODUCTION

The calibration or intercomparison of vacuum gages requires that they be subjected to an accurately known pressure of the calibration gas. The piston manometer (ref. 1) is intended to provide a means of creating and measuring this pressure. The particular manometer to be described in this report is for the range 10 to 700 microtorr (1 torr = 133.3 pascal). This report is concerned with the design of the manometer and its proof as a pressure-measuring instrument. The ion gage calibration problem is also treated because it affects the test and use of the manometer. The report is an amplification of some of the material in reference 1 and includes some more recent results.

Brombacher (refs. 2 to 4) has reviewed most of the various calibration methods that were described before 1965. In addition to the use of reference gages such as liquid manometers of the oil-U-tube and McLeod types, practical indirect methods are categorized in reference 4 as volumetric pressure dividers (volume-ratio methods), rate-of-pressure-rise methods, or conductance pressure dividers. Holanda (ref. 5) lists newer volume-ratio methods and also shows the accuracies of several modern volume-ratio calibration systems.

Like the three categories of indirect methods, the piston manometer depends on the ability to create a pressure that is almost two decades lower than the lower limit of the useful calibration range. Also, like the rate-of-pressure-rise and conductance-pressure-divider methods, it is used in a continuous-flow system. However, unlike these other two methods, it does not rely on the accurate computation or measurement of the conductance of a flow restriction. It yields a pressure from direct measurement of force and area, rather than inferring it from formulas for gas flow. Hence the nature of the flow regime (continuum, intermediate, or free-molecule) need not be known. The volume-ratio methods share this independence of Knudsen number.

The principle of measuring the force on a freely floating piston, while gas flows steadily through the gap between piston and surrounding cylinder, has been the basis of several measuring devices. A piston manometer for the millitorr range was described in 1955 (ref. 6); an inaccuracy of less than 1 percent was obtained in the range 0.5 to 20 millitorr. Devices for the continuum-flow regime, which measure low differential pressures at an absolute level of 1 bar (10^5 Pa), range from early instruments (ref. 7), variations of which are still in commercial use today, to present-day commercial precision pressure calibrators. Reichardt's manometer (ref. 7) had a differential-pressure range of the order of 1 millitorr. Modern precision dead-weight devices have inaccuracies of a few hundredths of 1 percent for ranges exceeding 15 torr. Brombacher (refs. 2 and 3) lists related devices.

A principal area of application of the piston manometer described here is the calibration of ion gages. Ion gages are also used to measure the pressure on the downstream side of the piston. They were also used to test the manometer and establish its probable error. Because of this prominence of the ion gage, it is important to state explicitly the assumptions made concerning characterization and calibration of such a gage. For concreteness, the assumptions will be enumerated for the particular case of a tubulated gage. These assumptions are:

(1) A particular gage consists of a specified mechanical arrangement of electrodes and their envelope, a specified set of potentials applied to the electrodes or of currents passed through them, a specified housing temperature, and a specified history of the gage. The specifications include the electrode and housing materials, especially the electron-emitting surfaces. Envelope temperature has usually been assumed to be adequately constant and not to require control, as long as the envelope is surrounded by

1-bar laboratory air and there is no forced convection. In order to eliminate variable effects of gage history, it has been customary to apply a standardized degassing procedure; such procedure is generally effective if the gage has only been subjected to relatively inert gases, but may be ineffective if the gage has previously been exposed to a highly active gas like oxygen.

Whenever any of these conditions is changed, the gage need no longer be expected to have the same calibration. It becomes a different gage.

(2) Calibration of a tubulated gage involves the creation of a known pressure in the plane of the mouth of the tubulation and a net flux of gas through this plane, which is preferably zero or, when zero flux is unattainable, is of a small, constant, and reproducible magnitude. In the second eventuality, the rate at which calibration gas is supplied must be large compared with the pumping speed of the gage. This gage pumping speed may be on the order of 0.1 liter per second (ref. 8).

(3) Ideally, only the calibration gas is to be present at the mouth of the tubulation. If other, contaminating gases are present, as occurs in practice, their identities and partial pressures must be known sufficiently well to permit adequate correction for their presence.

THEORY OF THE PISTON MANOMETER

Basic Arrangement

Figure 1 illustrates the arrangement of apparatus, the calibration technique, and the piston manometer concept. The baseplate of a conventional bell-jar type pumping system carries a calibration ring on which the gages to be calibrated are mounted. The glass bell jar rests on top of the ring. Gage tubulation axes are horizontal, radial, and substantially coplanar.

The centrally located baseplate opening through which the bell jar would ordinarily be evacuated is almost blocked by a piston in the form of a lightweight horizontal disk. The piston is suspended from a downward-force measuring device (dynamometer) and floats freely in the baseplate opening, with very small annular clearance. Piston area is about 100 square centimeters, so that 1 microtorr of differential pressure produces a force of 1.33 micronewtons (136 μg force).

Calibration gas enters at the top of the bell jar, at a rate controlled by a finely adjustable leak valve capable of sustaining a pressure drop of 1 bar. The gas is beamed upwards to facilitate uniform dispersal by the time it reaches the plane of the gage tubulations. All of the entering gas is removed through the annular gap between piston and the baseplate orifice. This gap is so small that there is a high ratio between upstream pressure p and downstream pressure p_0.

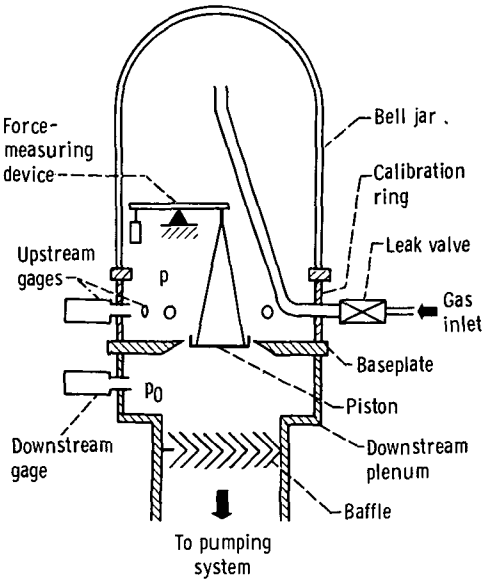

Figure 1. - Basic arrangement of piston manometer for vacuum-gage calibration.

A second chamber, of appreciable volume and cross section, is downstream of the baseplate orifice. A water-cooled baffle, which provides some minor advantages to be discussed later, is interposed between this downstream plenum and the pumping system. Ion gages measure the pressure p_0 in the downstream plenum.

The pumping system in the present apparatus uses an oil diffusion pump of nominal 25-centimeter diameter. It was chosen because it could provide steady pumping for all gases over thousands of hours, without attention. O-rings are used to seal between modular elements of the assembly, and a Viton L-ring is used to seal the glass bell jar.

The system design is intended to facilitate meeting the conditions of assumption (2) stated in the INTRODUCTION. Although there is steady flow from the top of the bell jar, the plane of the gage axes is sufficiently below the point of gas injection so that pressure in the plane is likely to be uniform. The piston is near this plane, so that its upper surface is likely to be at the same pressure. The annular gap constitutes a sufficiently small conductance (about 6 liter/sec in the present apparatus) to promote equalization of pressure in the cylindrical volume bounded by the calibration ring. For similar reasons, and partially because of the flow restriction provided by the downstream baffle (fig. 1), the downstream plenum is expected to be sufficiently isobaric so that the peripherally mounted ion gage adequately indicates the pressure on the underside of the piston. The temperature difference between the baffle and the piston produces negligible difference between pressure at the mouth of the downstream gage and pressure on the underside of the piston. The continuous mass flow of calibration gas through the annulus provides an acceptably large ratio of calibration gas to contaminating gases.

Basic Equations

If piston area is A and the net force on the piston due to pressure is ΔF, the upstream total pressure is given by

$$p = p_0 + \frac{\Delta F}{A} \tag{1}$$

(See appendix A for definitions of symbols.) If the pressure ratio p/p_0 were high, the accuracy of measuring p would depend principally on the accuracy of measuring force and area.

Ideally, both p and p_0 would be due solely to the calibration gas, and there would be no contamination due to permeation through gaskets or to desorption from gas sources in the upstream or downstream plenums. If G_a is the conductance of the annulus, $\dot{V}_0$ is the volumetric pumping speed in the downstream plenum, and the system is isothermal, conservation of mass would require that

$$(p - p_0)G_a = p_0\dot{V}_0 \tag{2}$$

so that

$$\frac{p}{p_0} = 1 + \frac{V_0}{G_a} \tag{3}$$

Thus, it is desirable that downstream pumping speed be high and that annulus width be small.

Although equations (2) and (3) represent only idealized conditions, where downstream contamination is absent, equation (1) is always true. In equation (1) the pressures p and p_0 are total pressures. They include the partial pressures of any contaminating gases introduced by permeation or desorption.

Downstream pumping speed $\dot{V}_0$ drops as p_0 approaches the ultimate pressure attainable in the downstream plenum. This ultimate pressure is determined by the amount of contaminants generated in the downstream plenum.

In the practical realization of the apparatus, effects of contamination were almost negligible at pressures above 100 microtorr, and the ratio in equation (3) was on the order of 200. At 10 microtorr, the effect of contaminants was appreciable, and the pressure ratio dropped to about 100. Thus, at $p > 10$ microtorr, a 20 percent error in knowledge of p_0 would produce no more than 0.2 percent error in knowledge of p, so

that the measurement of p depends principally on the accuracy of the force and area measurements.

The effects of contamination and of ultimate pressure may be clarified by considering a simplified electrical analog of the system.

Electrical Analog

Figure 2 is an electrical analog of the principal components of the system. In this representation, potential difference E may be set equal to pressure difference, current I to mass flow rate, electric resistance R to $\mathscr{R}T/M$ divided by vacuum conductance G (where M is molecular weight, T is absolute temperature, and $\mathscr{R}$ is the universal gas constant), and electric capacitance C to the product of chamber volume V and $M/(\mathscr{R}T)$. Equations of the electrical circuit will hold for the pneumatic system if analogous pneumatic quantities replace the electrical ones.

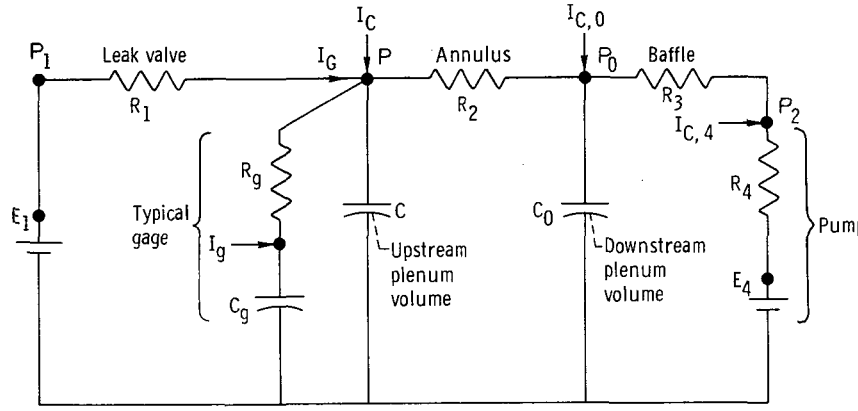

Figure 2. - Electrical analog of system of figure 1.

If T and M are constant everywhere, more convenient analogs are E to pressure difference, I to throughput (the product of volume flow rate and absolute pressure), R to the reciprocal of vacuum conductance, and C to chamber volume.

The flow of calibrating gas is represented by I_G. Influx of contaminating gases in the upstream and downstream plenum and at the pump mouth is shown as I_C, $I_{C,0}$, and $I_{C,4}$, respectively; flux in the gage envelope is I_g. The upstream current I_C merely raises the total pressure measured by the piston manometer. For facility of computation, the current I_g may be considered as slightly altering the value of I_C; hence, I_g will not appear explicitly in the following analysis.

Pressures at points P, P_0, P_1, P_2 are p, p_0, p_1, and p_2, respectively. Points

P and P_0 represent the locations of the upstream and downstream plenums, respectively. Point P_1 represents the inlet of the adjustable leak valve and point P_2 represents the vicinity of the mouth of the diffusion pump.

In the pressure range of interest in this report, the pumping system requires representation of the analog E_4 of pump fluid vapor pressure, the analogous resistance R_4 introduced by pump-entrance geometry, and the analog $I_{C,4}$ of contaminating gas flow originating at the pump entrance. However, the analysis is simplified by defining a potential difference E_{20} given by

$$E_{20} = E_4 + I_{C,4}R_4 \tag{4}$$

The analogous pressure p_{20} represents the pressure that would be present at point P_2 when I_G, I_C, and $I_{C,0}$ are each zero.

The reduction in vapor pressure that is effected by a cooled baffle cannot be rigorously represented by conventional symbols, but it is adequate to think of p_{20} as representing the pressure after cooling and to treat the baffle as a fixed resistance R_3.

Steady-state conditions. - In the steady state, the pressure p/p_0 is obtainable from figure 2 as

$$\frac{p}{p_0} = \frac{1 + \dfrac{I_{C,0}}{I_{GC}} + \dfrac{R_2}{R_{34}}}{1 + \dfrac{I_{C,0}}{I_{GC}} + \left(\dfrac{R_2}{R_{34}}\right)\left(\dfrac{p_{20}}{p}\right)} \tag{5}$$

where

$$R_{34} \equiv R_3 + R_4 \tag{6a}$$

$$I_{GC} \equiv I_G + I_C \tag{6b}$$

If $I_{C,0} \ll I_{GC}$, as is the case in the present arrangement of apparatus,

$$\frac{p}{p_0} \approx \frac{1 + \dfrac{R_2}{R_{34}}}{1 + \left(\dfrac{R_2}{R_{34}}\right)\left(\dfrac{p_{20}}{p}\right)} \tag{7}$$

It should be noted also that, in the present apparatus, $p_{20} \ll p$.

Equation (7) shows that the pressure ratio p/p_0 depends only on the resistance ratio R_2/R_{34} and on the pressure ratio p_{20}/p. As p increases, the ratio p/p_0 approaches an asymptote

$$\frac{p}{p_0} \rightarrow 1 + \frac{R_2}{R_{34}} \tag{8}$$

Two special cases are of practical interest.

Case I:

$$R_2 \gg R_{34}$$

This represents the case when the piston is in its normal position in the orifice. Then equation (7) should be used as it stands.

Case II:

$$R_2 \approx R_{34}$$

This represents the case when the piston is removed from the orifice so that flow can take place through the full area of the orifice. We denote the analogous resistance of the orifice as R_2^*. Then equation (7) becomes

$$\frac{p}{p_0} \approx 1 + \frac{R_2^*}{R_{34}} \tag{9}$$

Dynamic response. - When

$$R_1 \gg R_2 \gg R_{34} \tag{10}$$

and C_0 is only a small fraction of C, the time constant τ of response of the potential of point P to an abrupt change in E_1 or in R_1 is given very closely by

$$\tau = CR_2 \tag{11}$$

in electrical terms, or by

$$\tau = \frac{V}{G_a} \tag{12}$$

in pneumatic terms, where V is upstream-chamber volume and G_a is vacuum conductance of the annulus. Thus, a higher pressure ratio may be obtained by reducing annulus area (eq. (8)) but only at the expense of a higher time constant and increased time required to perform a multipoint calibration.

Drag Force

Most probable magnitude. - The flow of gas through the annulus produces a drag on the vertical sides of the disk-shaped piston. Because this drag force turns out to be only a fraction of 1 percent of the force ΔF that appears in equation (1), it is not necessary to compute it accurately. If simple bounds are put on the magnitude of drag force and the correction to ΔF is taken as the arithmetic average of these bounds, the resulting probable error in ΔF will be 1/4 of the difference between bounds - an acceptably small uncertainty.

The lower bound of the drag force is zero. This is the force that would be present if both piston and orifice were coplanar knife edges of zero thickness. The upper bound of the drag force is 1/2 of the product of annulus area A_a and pressure difference $p - p_0$. This is the drag force that would be present if both piston and orifice surfaces were elements of coaxial cylinders. Thus if radial annulus width is b and orifice diameter is D, the fractional correction for drag may be taken as $2b/D$ with a probable error of b/D.

Effective piston area. - A convenient way to apply this correction is to take the area A in equation (1) as equal to the area of a circle whose diameter is $D - b$. The geometric area of the piston is thereby augmented to allow for the most probable drag force. The correction is independent of the Knudsen number of the flow.

EFFECTS OF CONTAMINATING GASES IN ION GAGE CALIBRATION

Total pressure in the upstream plenum. - The sensitivity S_G of an ion gage to a calibration gas G will be defined as

$$S_G = \frac{\iota_G^+}{p_G} \tag{13}$$

where ι_G^+ is the measured collector current due to pressure p_G of the calibration gas. (The symbol G should be replaced by the chemical symbol for the particular gas.) This sensitivity is generally different for different gases. The definition of equation (13) is more convenient for the purposes of this report than the more common definition in which the right-hand side of equation (13) is divided by the electron current. The present form of the definition also parallels the definition of mass spectrometer sensitivity that will be presented later.

In a summary review of the literature up to 1966, Summers (ref. 9) shows that, for any particular gage, S_G is generally proportional to the peak total ionization cross section of the gas, or to its molecular polarizability. In additional work reported in 1972, Holanda (ref. 10) shows that Summers' conclusions apply to ion gages of the conventional-triode and Bayard-Alpert types but that there are more effective criteria for other types of ionization gages.

The definition given by equation (13) implicitly treats as part of the gage's characteristics the effects of any gas dissociation that may occur within the gage envelope or within the active volume of the electrode structure. The fact that such dissociation may occur suggests that, for active gases like H_2O, the sensitivity may be different for different filament materials. However, since p_G represents the pressure of the neutral gas at the mouth of the gage, the piston manometer should provide a correct measure of this pressure, if there are no foreign contaminating gases in the bell-jar volume.

If such contaminating gases exist and are assigned the running injex j, the following equations hold

$$\iota_C^+ = {}_C\sum \iota_j^+ \tag{14}$$

$$p_C = {}_C\sum p_j \tag{15}$$

$$S_G = \frac{\iota^+ - \iota_C^+}{p - p_C} \tag{16}$$

where ι^+ and p are the measured collector current and measured total pressure, respectively, when calibration gas is being injected, and ι_C^+ and p_C are the aggregate collector current and aggregate total pressure, respectively, due solely to the contaminating gases. The subscript C to the left of the summation sign indicates that the summation is over the totality of contaminants.

Such contaminating gases may come from three principal sources:

(1) Permeation and evolution of gas due to the presence of virtual leaks, polymeric gaskets, and desorbing surfaces. As a first approximation, the partial pressure p_C

and corresponding current ι_C due to these sources should be independent of the amount of calibration gas, so that these quantities become constant subtrahends in equation (16).

Incidentally, the measurements of current and pressure before opening the leak valve provide a means of determining S_C, the gage's sensitivity to the aggregate of contaminating gases, without knowing the identity of the contaminants

$$S_C = \left(\frac{\iota_C^+}{p_C}\right)_{p_G=0} \tag{17}$$

There is a possibility that, in a closer approximation, use of equation (16) with these initial values of ι_C and p_C may overcorrect when p increases, because the rate of desorption of some gases may decrease as bell-jar pressure increases. However, the numerical magnitude of the overcorrection is quite small, because the correction itself drops as p/p_C increases. The correction represented by ι_C^+ and p_C in equation (16) exists only when S_C is significantly different from S_G; the correction vanishes when $S_G = S_C$. This fact becomes more evident when equations (16) and (17) are combined to yield

$$S_G = \frac{\iota^+}{p - p_C\left(1 - \frac{S_C}{S_G}\right)} \tag{18}$$

Equation (18) is more convenient for computational purposes than equation (16) when a number of gages are being calibrated.

(2) Surface reaction of the contaminating gas with trace gases bound in hot surfaces, such as filaments, present in the upper plenum.

(3) Dissociation of the calibration gas by hot surfaces or electron beams present in the upper plenum. The gas at the mouth of the gage then is not solely the calibration gas G. In this case the simplified treatment that led to equation (18) is no longer adequate, and a more general treatment is required. This treatment draws no distinction between sources of contaminants.

Equations (14) to (16) are used, together with the definition

$$S_j = \frac{\iota_j^+}{p_j} \tag{19}$$

An independent estimate of the partial pressures p_j is required. Such an estimate is obtainable from a calibrated mass spectrometer whose sensitivity s_j is given by

$$s_j = \frac{y_j}{p_j} \tag{20}$$

where y_j is the output indication of the mass spectrometer produced by partial pressure p_j of the j^{th} gas. This output indication may be taken either as (a) the height of the principal peak, (b) the height of some other distinctive peak, or (c) the sum

$$\sum_k y_{j,k}$$

of the heights of k peaks that appear when the j^{th} gas is injected. The selection of which of these definitions is to be used depends on the user's intuition of which representation is likely to be more unequivocally proportional to p_j. When the cracking pattern of the mass spectrometer for the j^{th} gas is invariant and there are no coincident peaks due to other gases, each definition will yield the same result.

Use of equations (14) to (16) and (19) and (20) yields the following statement of S_G in terms of measured quantities and of the ratio S_j/S_R, where subscript R denotes some reference gas for which gage sensitivity is known:

$$S_G = \frac{\iota^+ - S_R \sum_C \left[\left(\frac{S_j}{S_R}\right)\left(\frac{y_j}{s_j}\right)\right]}{p - \sum_C \frac{y_j}{s_j}} \tag{21a}$$

If the reference gas is the calibration gas itself, the equation takes the simpler form

$$S_G = \frac{\iota^+}{p - \sum_C \left(1 - \frac{S_j}{S_G}\right)\frac{y_j}{s_j}} \tag{21b}$$

The ratio S_j/S_R may be taken from reference 9, if it has not been currently measured for the principal contaminants. Since the summations in equations (21a) and (21b) represent small corrections, when p_C is small compared with p, an appreciable uncertainty in knowledge of S_j/S_R will produce little uncertainty in knowledge of S_G.

Equivalent indicated gas pressure. - The preceding discussion indicates that when an ion gage, having sensitivity S_G for gas G, is used to measure the pressure p of a gas containing contaminants, the gage actually indicates the equivalent indicated pressure p_{EIG} of gas G given by

$$p_{EIG} = \frac{\iota^+}{S_G} = p - \sum_C \left(1 - \frac{S_j}{S_G}\right) p_j \tag{22}$$

(The letter G is to be replaced by the chemical symbol for the gas.)

This relation will be used to convert the readings of the downstream ion gages to an equivalent downstream pressure.

Total pressure in the downstream plenum. - The total pressure p in the upstream plenum is correctly measured by the piston manometer even when contaminating gases are present. However, since an ion gage is used to estimate the total pressure p_0 in the downstream plenum, the conversion from measured collector current ι_0^+ to pressure p_0 requires correction for the presence of contaminating gases. Fortunately, this correction need not be precise because p_0 need not be known accurately when the piston manometer is used in the range where $p >> p_0$.

Two alternative methods may be used for computing p_0.

Method 1: Inversion of equation (22) leads to

$$p_0 = \frac{\iota_0^+}{S_G} + \sum_C \left(1 - \frac{S_j}{S_G}\right) p_{j,0} \tag{23}$$

This equation may be used if the sensitivity S_G of the downstream gage is known, if S_j/S_G is obtainable from reference 9 or from superior information and if the downstream partial pressures $p_{j,0}$ are assumed to be p_0/p times the upstream partial pressures p_j determined from a calibrated upstream mass spectrometer. Use of equation (23) may be necessary when there is dissociation of the calibration gas.

Method 2: If the sources of contamination are principally permeation and desorption, rather than dissociation, equations (17) and (18) may be used to yield

$$p_0 = \frac{\iota_0^+}{S_G} + \left(1 - \frac{S_C}{S_G}\right) \frac{\left(\iota_{C,0}^+\right) p_{G=0}}{S_C} \tag{24}$$

Both methods require some iteration, because a preliminary estimate of S_G is needed.

PRACTICAL DESIGN

The design of the apparatus outlined in figure 1 was intended to provide a proof of the piston manometer by identifying limitations on its performance. A principal testing tool was the exercise of actually calibrating some ion gages. However, convenience of gage calibration was secondary to simplicity of system design that would help to understand the factors affecting piston-manometer performance.

A photograph of most of the apparatus above the baseplate is shown in figure 3. Construction details are arranged to minimize virtual leaks. Contacts between ordinarily flat surfaces are replaced by point or line contacts, following the principles of kinematic design (ref. 11). Flats are milled on the sides of screws and of circular rods that fit into holes, in order to facilitate gas passage. Blind holes are avoided.

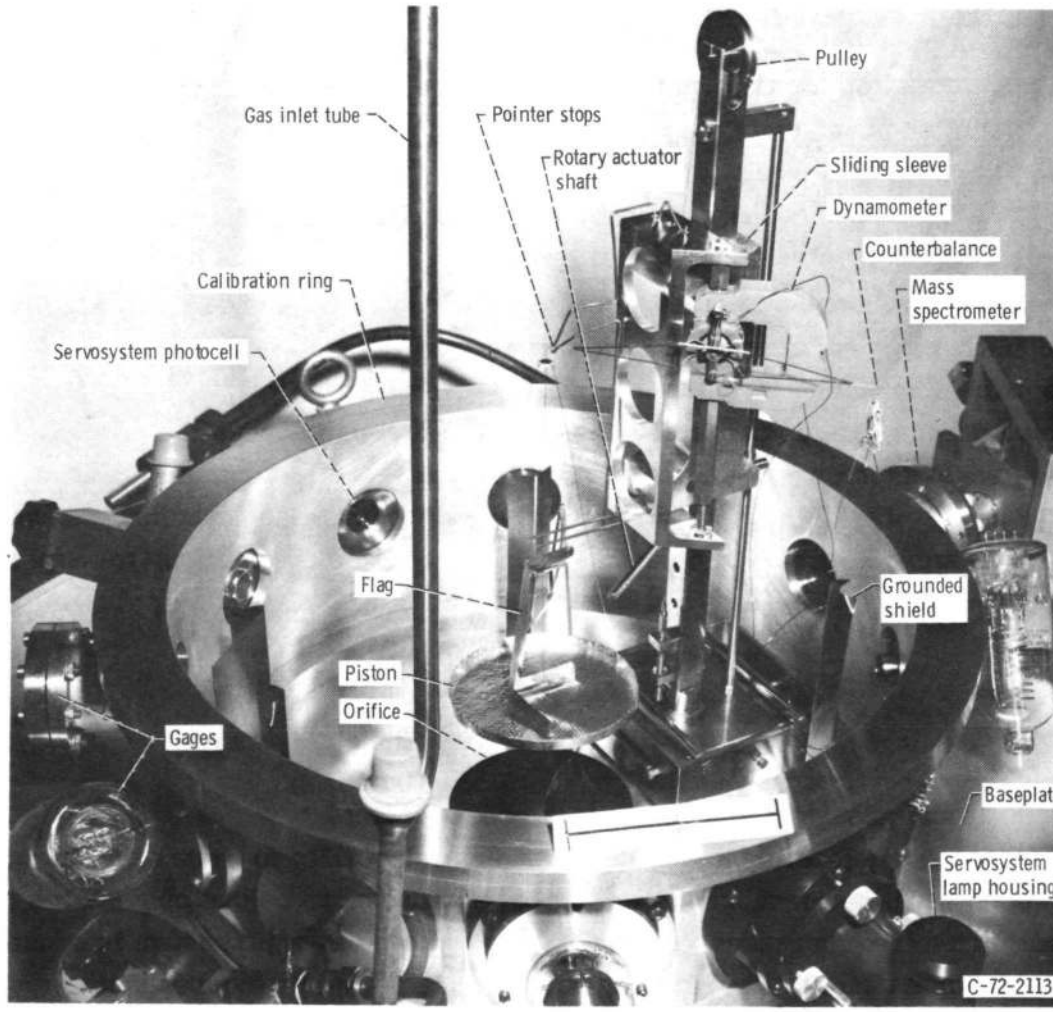

Figure 3. - Photograph of most of apparatus above baseplate.

Downstream System

The downstream system includes the pumping system, downstream plenum, and downstream gages. The pumping system uses a 25-centimeter diffusion pump with central cold cap and a water-cooled chevron baffle above it (R_3 in fig. 2). Only a water-cooled baffle is interposed between the diffusion pump and the mechanical forepump. The downstream plenum between the baffle and the baseplate is about 29 centimeters in diameter by about 10 centimeters high. Two Bayard-Alpert type gages are inserted through the sides of the plenum, with tubulation axes radial. O-ring seals are used between pump, baffle, plenum, and baseplate.

Baseplate and Orifice

The baseplate is an aluminum plate, 3 centimeters thick and 60 centimeters in diameter, that is centered over the downstream plenum. The central orifice is knife-edged, as shown in figure 4, with a nominal area of 100 square centimeters. However, to assure roundness and accurate definition of diameter, the knife edge is beveled to provide a cylindrical surface 0.1 millimeter high.

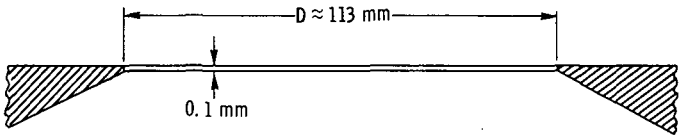

Figure 4. - Baseplate orifice.

Piston

Piston design is intended to provide minimum weight, with adequate stiffness to define and retain a precise area. Design of the piston and its suspension are shown in figure 5. The piston is made of 20-micrometer-thick aluminum foil and is formed into a shallow pan with vertical sides about 0.6 centimeter high. The outside diameter of about 11.3 centimeter is intended to provide an annulus of about 0.2 millimeter radial width between piston and orifice. Thus, annulus area should be on the order of 0.7 percent of piston area.

The method of forming the piston is described in appendix B. The forming produces wrinkled vertical surfaces, since the foil is folded over on itself. This structure is too flimsy to permit direct mechanical measurement of area, but the effective piston area can be deduced from the orifice area, which is mechanically measurable, by techniques described under TESTS AND RESULTS.

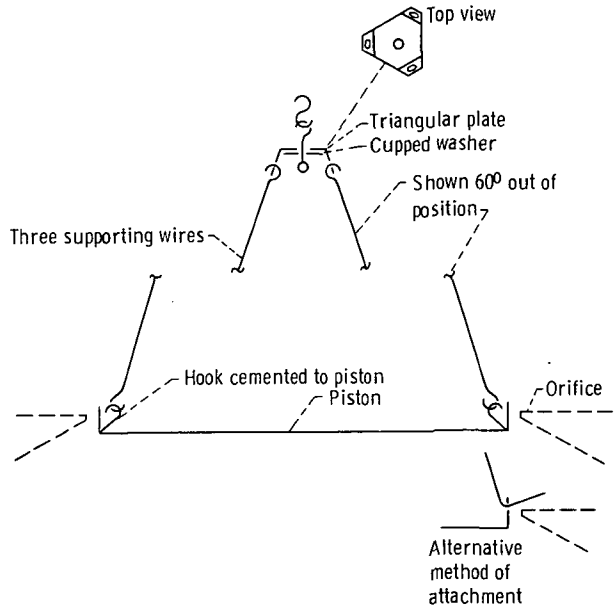

Figure 5. - Piston and its suspension.

The piston is supported from three wire hooks cemented to the inside corners of the pan, at 120° intervals. Wires (20 cm long) lead to an upper triangular plate, which is supported from a central supporting wire so that the assembly can pivot freely about this wire.

An alternate mode of supporting the piston, also shown in figure 5, is to hook the 20-centimeter wires through 0.3-millimeter-diameter holes punched in the vertical side of the dish, about 0.2 centimeter from the upper edge. An advantage of this mode of support is that the protruding wires keep the dish from falling through the hole, but there is a loss of ruggedness in comparison with the cemented-hook technique. All wire elements are of 0.2-millimeter-diameter constantan.

The overall height of the suspension is deliberately made large so that failure to center the piston perfectly in the orifice will result in a very small horizontal force between the side of the piston and the edge of the orifice. Then, when flow is taking place through the annular gap, the piston swings horizontally within the clearance area, in a random manner, so that there is negligible net vertical force of friction.

Dynamometer

The force-measuring device is a d'Arsonval galvanometer element with conical pivots on a horizontal axis. A schematic outline of its configuration is shown in figure 6. Two stiffened pointers, 180° apart, create the appearance of an equal-arm balance. The

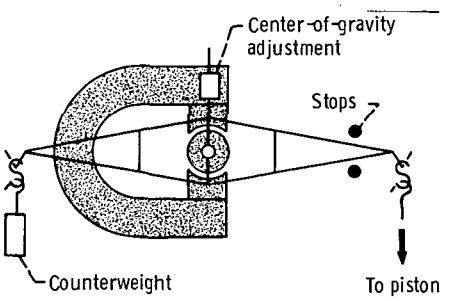

Figure 6. - Dynamometer.

piston is suspended from one pointer tip and counterbalancing aluminum weights from the other. Stops, about 3 millimeters apart, prevent excessive deviation from the horizontal position. When the piston is centered between stops, it is also vertically centered within the baseplate orifice, as shown by the dotted outline in figure 5. When there is a downward force on the piston, current through the galvanometer coil is adjusted to keep the pointer centered between the stops. A vertical rod, attached to the pointer and extending upward, carries a sliding weight that is adjusted to raise the center of gravity until the movement is marginally stable. Thereby, almost the same current is required to keep the pointer anywhere between the stops. The direct current (dc) required to maintain this approximately centered position becomes an accurate measure of the downward force on the piston. A 60-hertz dither current is also injected to overcome pivot friction.

Natural period of the assembly is 8 seconds. Spring constant is equivalent to not more than 0.2 microtorr per millimeter deflection of the pointer tip. Total weight on the pivots is 1.6 grams.

In an early version of the instrument, coil current was controlled manually by adjusting a multiturn rheostat-potentiometer connected to a regulated dc power supply, while piston position was observed visually. In this version the alternative protruding-hook method of piston support shown in figure 5 was efficacious in preventing catastrophic downward excursion of the piston. The stops shown in figure 5 were absent, so that, by appropriate current adjustment, the piston could be elevated about 5 centimeters above the orifice. The bell jar could then be evacuated at high speed.

In the present version of the instrument, an optical servosystem is used to control piston position automatically. The cemented-hook method of piston support shown in figure 5 is used. There is a slight improvement in accuracy, over the older system, and a great improvement in convenience. It is also possible to follow a continuously changing pressure.

Servosystem

Principal optical elements of the servosystem are shown in figure 7. The image of a straight horizontal-wire filament of an incandescent lamp is focused about 10 centimeters above the center of the piston. A photovoltaic cell receives radiation from the lamp; the lens in front of this cell is focused on the lamp condensing lens. A flag, resting on the upper surface of the piston, has a horizontal edge that half-intercepts the filament image when the piston is properly positioned vertically. A vertical motion of 0.3 millimeter is sufficient to produce a change from complete illumination to complete extinction. Lamp and photocell assemblies are outside the vacuum system and are mounted at opposite ends of a diameter of the calibration ring. Light is transmitted through O-ring sealed windows.

The flag is made of 20-micrometer-thick aluminum foil; its configuration, shown in figure 7, is such as to impart adequate structural rigidity. The flag also has a second horizontal edge, about 10 centimeters below the principal one, that is used for making a

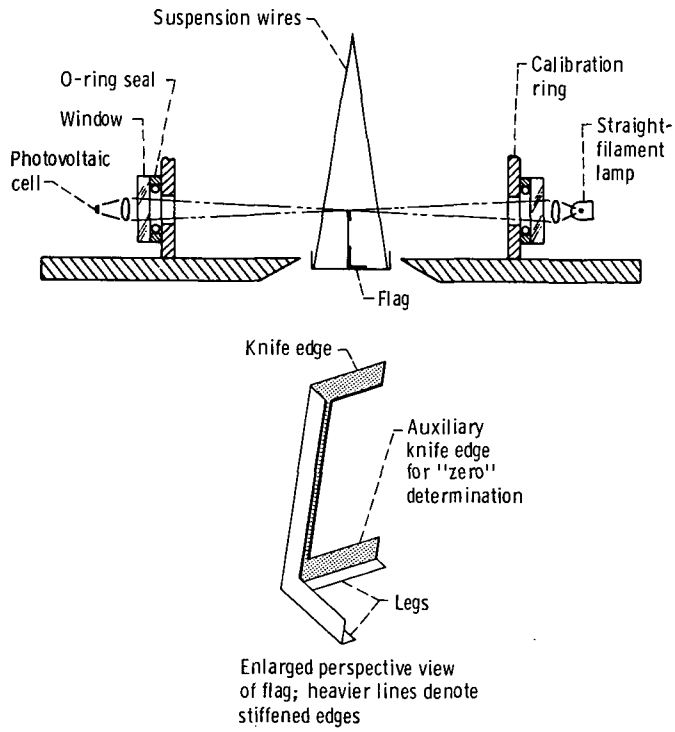

Figure 7. - Optical elements of servosystem.

dynamometer-zero measurement, as will be explained in a later section. Shifting of the flag on the surface of the piston has been prevented by either of the following expedients: (1) two U-shaped wire staples driven through the flag and piston or (2) a drop of high-vacuum epoxy cement at each of two locations.

The servosystem's electrical circuit is shown in figure 8. A photocell bias adjustment provides fine control of the vertical position of the piston. A lag-compensating network provides dynamic stabilization. A 60-hertz dither current overcomes pivot friction. A precision shunt resistor provides a means for measuring dynamometer-coil current with an integrating digital voltmeter (IDVM).

Since the servosystem has less than 100-percent feedback, there would be a slight progressive change in the vertical position of the piston as pressure increased. A manually adjusted reset circuit prevents this by permitting 100-percent feedback, as indicated by the null indicator at the amplifier output. This meter incidentally provides a sensitive indication of the piston's vertical position.

The manual reset circuit also provides a means of manually controlling the dynamometer current when the servosystem circuit is disconnected. Such manual control is used in calibration of the dynamometer and also to keep the piston vertically centered when the

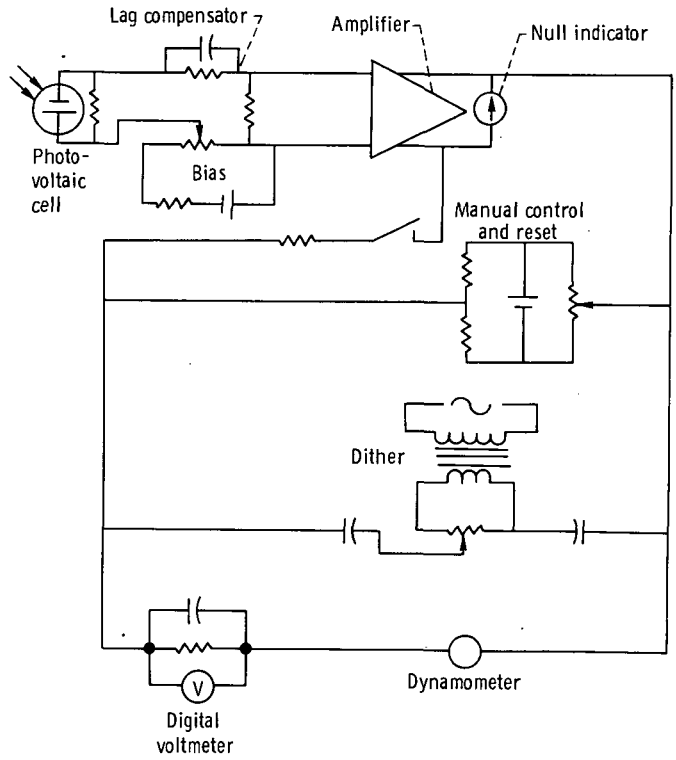

Figure 8. - Electrical circuit for control of dynamometer current. Regulated power supplies are symbolized by batteries.

equipment is in a standby condition. These operations will be described in the section Operating Procedures.

The servosystem, with reset, maintains the piston's mean vertical position constant to 0.1 millimeter. However, the dynamic behavior of the system is imperfect, and there are random vertical oscillations, aggravated by the dither current, that show up as fluctuations about the mean dynamometer current. These fluctuations are centered at about 9 hertz and have an rms amplitude that varies from 1 percent at 10 microtorr to 1/4 percent at 500 microtorr. A 10-second IDVM integration time is used to reduce the average-current measurement error that may be caused by these fluctuations.

Dynamometer Support

The dynamometer is carried on a sleeve that can slide along a vertical rod, 2.5 centimeters in diameter, affixed to a base that can be properly positioned on the baseplate. The sleeve has a yoke that straddles a guide rod parallel to the main vertical rod in order to prevent sleeve rotation. Figure 9 is a simplified schematic representation of the arrangement. Adjusting screws permit fine horizontal positioning of the piston. Elevation of the sleeve can be effected by turning a rotary actuator, mounted on the calibra-

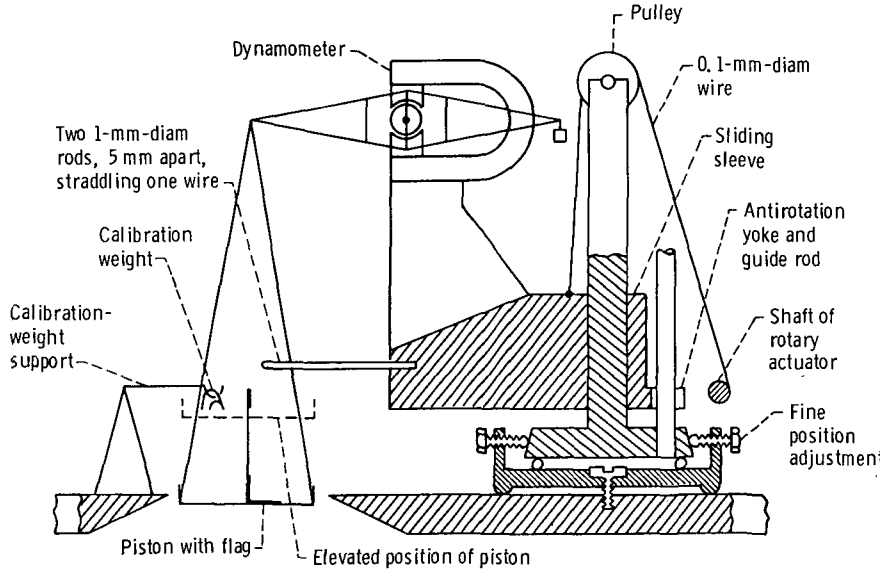

Figure 9. - Dynamometer support.

tion ring, around whose shaft is wrapped a wire that runs over a fixed pulley and is attached to the sleeve.

In order that the flag knife edge remain approximately normal to the optical line of sight of the servosystem, excessive rotation of the piston must be prevented. To this end, two parallel 1-millimeter-diameter rods extend horizontally from the side of the sleeve, so that they straddle one of the three long suspension wires with about a 5-millimeter clearance.

A wire weight, of about 30-milligram mass (equivalent to about 200 microtorr), is suspended above the piston from the hooked end of a tripod that rests on the baseplate. When the piston is elevated to a sufficient height, the weight rests entirely on the upper surface of the piston and is lifted off its supporting hook. The mass of this weight is known to a probable error of 0.04 percent. Its use permits determination of dynamometer sensitivity while the bell jar is evacuated.

Calibration Ring

The calibration ring of the present assembly has 12 ports. Two diametrically opposite ports are used for the optical elements of the servosystem. Other ports are used for the dynamometer-elevating actuator, the calibration-gas inlet, a leak-detector connection (with shutoff valve), and a connector for the dynamometer-coil leads. For the present tests, one port holds a 60° sector type mass spectrometer with nude ion source, and the five remaining ports hold ion gages to be calibrated. A special method of attaching tubulated ion gages allows the 14-millimeter-diameter tubulations to project 28 millimeters from the inside wall of the calibration ring. Sheet stainless-steel baffles, resting on the baseplate, are placed about 40 millimeters in front of each of the gages in order to prevent line-of-sight transfer of neutral or charged particles between gages; these baffles constitute ground-potential surfaces. The efficacy of these baffles is demonstrated by the discoloration that appears on them in front of the gage mouth, after protracted exposure.

Operating Procedures

Initial evacuation and standby. - Evacuation of the bell jar from atmospheric pressure is performed with the piston elevated 10 centimeters above the baseplate orifice. To prevent violent air currents that would damage the suspended piston, evacuation is performed slowly, through a needle valve with 1.5-millimeter-diameter opening, until the pressure is less than 10 torr; about 10 minutes are required.

The standby condition, when no calibration is being performed, is also with the piston 10 centimeters above the orifice, so that the bell jar is being pumped on at maximum possible pumping speed (about 1200 liters/sec of air).

Dynamometer calibration. - While the piston is in the raised position, it can be moved until the lower horizontal edge on the flag intercepts the servosystem light beam. The dynamometer pointer is centered between the stops. A "zero" or tare reading of dynamometer current is then taken, corresponding to the condition $\Delta F = 0$.

To determine sensitivity (mean slope of the curve of force against current) the piston is raised further until it completely supports the calibration weight. The dynamometer current is then adjusted manually until the pointer is centered between the stops. Since the calibration weight is large, the increased error due to use of manual rather than automatic balance is negligible.

Such determinations of zero and sensitivity are usually made before and after a gage calibration.

Ion gage calibration. - With leak valve closed, the piston is lowered into its proper position in the orifice and pressures are allowed to stabilize. The upstream pressure p_C and corresponding gage currents ι_C^+, due to contaminants, are read; S_C (eq. (17)) can be computed. The leak valve may then be opened to create higher pressures. For relatively inactive gases, like N_2 and the inert gases, equation (18) is adequate for computing sensitivity, since the total pressure p_C of contaminants does not appear to vary appreciably with total pressure p, as deduced from mass-spectrometer indications.

After an abrupt change in setting of the leak valve, there is an exponential change of pressure with a time constant of about 23 seconds. Thus, at least a 3-minute interval should elapse before pressure may be expected to have stabilized within 0.1 percent.

Standard commercial control units are used as regulated power supplies for the ion gage electrode potentials, but these control units are not used to measure ι^+ or ι^-. Ion gage collector current ι^+ is measured by measuring the voltage drop across a 10-kilohm resistor in series with the collector lead. Grid current ι^- is measured by measuring the drop across a 100-ohm resistor in series with the grid lead. Both voltages are measured with an IDVM having a 1-second integration period and a floating, guarded input. This IDVM is sequentially switched to the several gages being calibrated. Three seconds are allowed to elapse after switching, before a reading is actually recorded, in order to allow switching transients to expire. These transients, which are apparent only occasionally, are probably due to the capacitance of the ion gage power supplies, and imperfections in the guarding procedure. While these readings are being taken, several readings of dynamometer current are taken with a second IDVM having a 10-second integration period. Since the measurements of dynamometer current and of the gage currents are concurrent, the first-order effect of any slow drift in pressure is nullified.

To correct for slight variations in grid current ι^- that occur during the course of a

protracted calibration, the measured collector current is multiplied by the normalizing factor

$$\frac{\iota^-_{nom}}{\iota^-}$$

where ι^-_{nom} is the nominal grid current.

TESTS AND RESULTS

Pumping System Characteristics

The ultimate pressure p_0 in the downstream plenum, when no calibration gas was being injected, was about 0.1 microtorr. This was also the upstream-plenum pressure when the piston was out of the orifice (standby condition). When the piston was positioned inside the orifice, upstream pressure reached the steady-state value of about 4 microtorr, the residual contaminating-gas pressure p_C. The corresponding contaminating-gas throughput is about 20 torr liters per second. The mass spectrometer indicated that the principal contaminants were H_2O and CO.

Dynamometer Characteristics

The dynamometer's current-against-force calibration was determined with class S weights. These have a limit of error of (4 micrograms plus 0.07 percent), which is equivalent to (0.03 microtorr plus 0.07 percent). No systematic nonlinearity could be detected.

The calibration weight (fig. 9) used to check sensitivity was measured with the class S weights by the method of substitution. However, the absolute accuracy of the weight is not relevant to checking the consistency of calibration results, to which this report is confined; only the constancy of sensitivity is important. The peak-to-peak variation in this sensitivity over a 100-day period was 0.07 percent.

The zero readings, corresponding to $\Delta F = 0$, at the beginning and end of an 8-hour calibration run usually disagreed. The most extreme difference ever encountered was equivalent to 0.7 microtorr. For calibration purposes, the zero was assumed to change linearly, with time, from its initial to its final value. However, for the purpose of conservatively estimating the probable error in knowledge of zero, one fourth of the peak difference will be assumed, namely, about 0.2 microtorr. The reason for this large un-

certainty is not understood. The direction of the 1-day drift was not always the same. Nor was there any noticeable systematic drift of the daily average over a 2-month period; the peak-to-peak variation over this 2-month period was 1 microtorr.

Pressure Ratio

The measured pressure ratio p/p_0 is shown in figure 10 as a function of total pressure p. This curve is accurately represented by equation (7) if one takes

$$\frac{R_2}{R_{34}} = 238$$

and

$$p_{20} = 0.06\ \mu\text{torr} \tag{25}$$

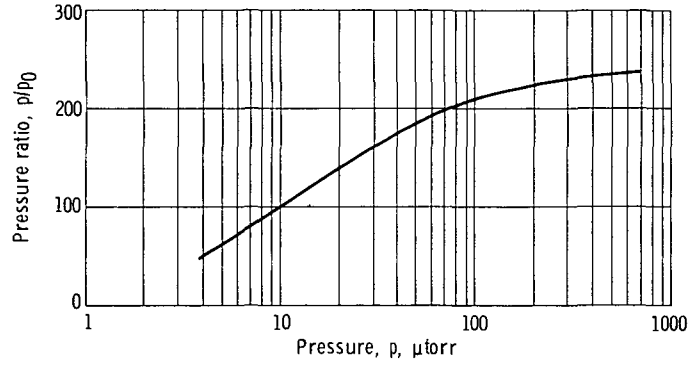

Figure 10. - Pressure ratio across the piston.

Downstream-Pressure Measurement

Downstream pressure is measured with two Bayard-Alpert-type gages of the same model. (As in ref. 9, "model" refers to a particular model number of a particular manufacturer.) These gages had not previously been calibrated. Two other gages of the same model were, however, calibrated in the upper plenum. The ratio between the readings of the two downstream gages was 1.32 at all pressures. The ratio between the readings of the two upstream gages was 1.22. It will be assumed that the mean value of the sensitivities of the downstream gages is the same as the mean value of the sensitivities of

the upstream gages. The probable error involved in this assumption is about 10 percent. Since (from fig. 10) the pressure ratio p/p_0 is about 100 at $p = 10$ microtorr, the corresponding probable error in p at $p = 10$ microtorr is about 0.1 percent. The error would have been negligible if calibrated gages had been used downstream.

Effective Piston Area

The piston is too flimsy to allow direct measurement of its diameter. A lower limit of diameter may be taken as the measurable diameter of the cylindrical anvil around which it is formed (appendix B) augmented by twice the thickness of the foil material of the piston. A more accurate determination of effective diameter $D - b$ is obtained from direct measurement of orifice diameter D with mechanical gages and an estimate of annulus width b. This estimate can be obtained in two ways.

Time-constant method. - Equation (12) may be applied by measuring the time constant of response of pressure to an abrupt change in leak valve setting or to upstream pressure (at P_1 in fig. 2). Upper-plenum volume was calculated from geometric measurements to be 125 liters. Annulus conductance may be taken as

$$G_a = Kv_a \cdot \frac{\pi Db}{4} \tag{26}$$

where πDb is geometric area of the annulus, v_a is average molecular speed, equal to $4\sqrt{\mathscr{R}T/(2\pi M)}$, and K is Clausing's correction factor (refs. 12 and 13) for the nonzero ratio of orifice-edge thickness to annulus width. Experimental measurements with argon yielded a value of $\tau = (23 \pm 3)$ seconds, leading to an annulus conductance of 5.4 liters per second and $b = 0.20$ millimeters.

Pressure-ratio method. - Equation (8) may be used to determine the ratio R_2^*/R_{34} when the piston is removed from the orifice, a high flow rate of calibration gas is maintained, and gages of the same model are used to measure both upstream and downstream pressures so that the measured current ratio ι^+/ι_0^+ may, to a first approximation, be assumed to equal the pressure ratio p/p_0. This experiment was performed, and R_2^*/R_{34} was determined to be 1.23 ± 0.11.

Since the pressure ratio R_2/R_{34} was 238 and since the conductance of a 100-square-centimeter orifice is 1000 liters per second for argon, it follows that R_2 should represent a conductance of 5.2 liters per second, corresponding to $b = 0.19$ millimeters.

The two methods of estimating b agree well within the extent expected from the uncertainties in the experimental measurements. Since the area correction involved is only of the order of 0.4 percent, the disagreement is acceptably small.

Random Error in Pressure Measurement

In addition to the enumerable errors previously discussed, one would expect to find additional random errors whose origin is not precisely definable. These will vary randomly with time, as distinguished from time-independent errors like the uncertainties in area or dynamometer sensitivity. One may speculate that one such error source might be the conversion of dynamometer current to the corresponding mean pressure difference $p - p_0$ through imperfect operational procedures or imperfect integration of fluctuating pressures, forces, or currents.

An estimate of such random errors was obtained from the following experiment. The exercise of calibrating several ion gages was performed by progressively opening the leak valve (fig. 1) to create a number of pressure steps that were fairly uniformly distributed on a logarithmic pressure scale and that occurred at relatively short intervals. Ion gage sensitivity was plotted against pressure and a smooth curve was drawn through the points. The random deviations of the individual points from the smooth curve were taken to represent the random error referred to previously. This interpretation is based on the postulate that the ion gage itself is an inherently smooth transducer of pressure to current, over a relatively short time interval. In this analysis, the absolute accuracy of the mean curve is of no interest; only short-term deviations from the smooth curve are of interest.

Five ion gages were calibrated simultaneously. Two were conventional triode type gages of the same model, with tungsten filament, glass envelope, and a 14-millimeter tubulation in line with the gage axis. Two were Bayard-Alpert-type gages with thoriated iridium filament, glass envelope, and 14-millimeter tubulation at right angles to the gage axis. The fifth gage was a Bayard-Alpert type with tungsten filament, stainless-steel envelope, and a 50-millimeter-diameter opening at one end that was almost flush with the wall of the calibration ring.

All gages received their potentials from commercial control units. The triode gages were operated at a collector potential of -20 volts, a grid potential of +150 volts and a grid current of 5 milliamperes. The Bayard-Alpert gages were operated at a collector potential of -30 volts and a grid potential of +150 volts. (All potentials are relative to the filament.) Grid current was either 1 or 10 milliamperes, except that the higher current was never used at pressures above 150 microtorr. As explained in the INTRODUCTION, a gage tube operated at 1 milliampere is considered a different gage than the same tube operated at 10 milliamperes.

The control unit electrometer remained connected to the gage, but the range switch was left at the highest pressure range setting, so that the input resistor remained unchanged throughout a calibration. Thus, there were no abrupt changes in electrical circuitry as the entire pressure range was covered, other than those due to switching of the IDVM to the various channels, as described under Ion Gage Calibration. However, the

emission-current rheostat was adjusted occasionally, when ι^- was about to drift more than 2 percent from its nominal value.

Preliminary runs with the mass spectrometer established that, when argon was the calibration gas, the partial pressure of contaminating gases remained substantially constant, so that equation (18) could be used to compute sensitivity. The contaminating gases were principally H_2O and CO.

Figure 11 shows results for five gages in the range 4.4 to 120 microtorr. The abscissa has been taken as p_{EIAr} as defined by equation (22) because this choice eases the

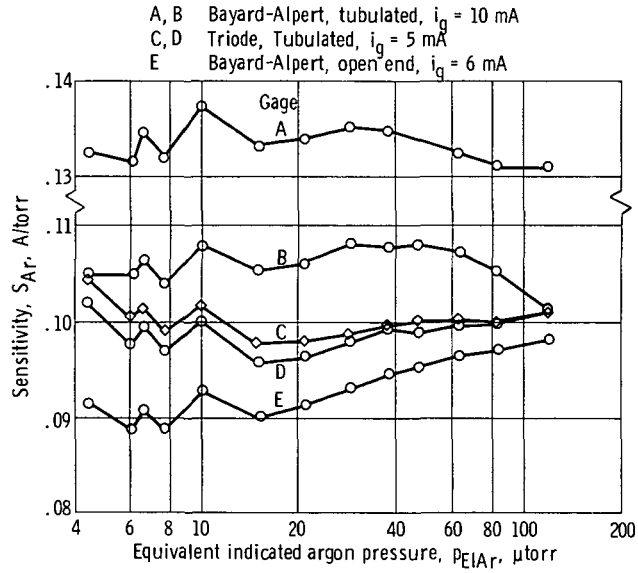

Figure 11. - Random variation in indicated argon sensitivity for various gages.

problem of deciding on the shape of the most probable mean curve at the lower pressure - the curve should be horizontal. Use of total pressure p rather than p_{EIAr} would not alter the conclusions. The readings at the lowest pressures have little meaning as far as gage sensitivity is concerned, because the gas consisted principally of contaminants, but the data remain useful in establishing deviations from a smoothed curve. Successive individual points have been joined by straight lines.

At the lower pressures, the congruence among the separate graphs is striking. Such congruence implies some factor common to all the graphs. We attribute this, conservatively, to the inability of the piston manometer to provide a correct measurement of total pressure. Other common factors, like changing gas composition, are considered less likely to produce the random pattern.

Figure 12 repeats the graph of figure 11 for one of the triode gages and extends it to the upper calibration limit of 700 microtorr. The dashed curves show how the mean

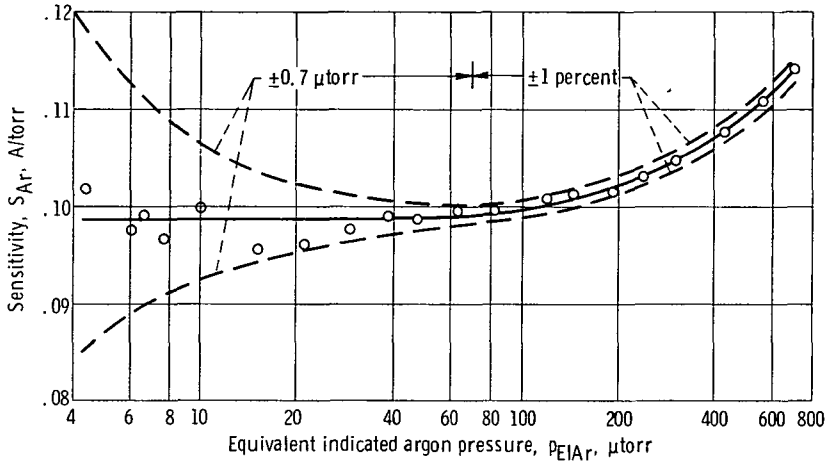

Figure 12. - Error bounds of typical gage calibration.

curve would change if the measured value of total pressure p were altered by the amount shown in the figure.

Similar curves have been drawn for the other gages that were calibrated. Results show that 90 percent of all points lie within the boundaries

$$\pm 0.7 \ \mu\text{torr for } 4.5 < p_{EIAr} \leq 140 \ \mu\text{torr}$$

$$\pm 1 \text{ percent for } 140 \leq p_{EIAr} < 700 \ \mu\text{torr}$$

All points lie within the boundaries

$$\pm 1 \ \mu\text{torr for } 4.5 < p_{EIAr} < 100 \ \mu\text{torr}$$

Summary of Errors

The table on page 29 is a listing of estimated probable errors that enter into total-pressure measurement by the piston manometer, in accordance with equation (1). Some errors have a truncated Gaussian distribution, others a uniform distribution. In any case, there is at least a 90 percent probability that an error will be less than twice the probable error.

The root-mean-square summation of errors leads to a value of ±(0.5 microtorr + 0.6 percent) in the measurement of total pressure. Computation of gage sensitivity through equation (16) entails errors in measurement of both p and p_C. The probable error in net pressure $p - p_C$ is then $0.5\sqrt{2}$ microtorr. Thus, when the calibration gas

Origin of error	Probable error
Downstream pressure, p_0:	
(1a) Calibrated gages	Negligible
(1b) Uncalibrated gages of a calibrated type	10 percent of p_0
(2) Effect of contaminants	0.02 μtorr or 20 percent of p_0
Effective piston area, A:	
(3) Orifice diameter	Negligible
(4a) Annulus gap	15 percent of gap area
(4b) Frictional drag	25 percent of gap area
(4c) Combination of 4a and 4b	0.2 percent of A
Net force, ΔF:	
(5) Dynamometer sensitivity	Negligible
(6) Dynamometer zero drift	0.2 μtorr
(7) Random error in current-to-pressure conversion	0.4 μtorr or 0.5 percent of p

is inert, the error in calibration-gas pressure (denominator of eq. (16)) is equal to ±(0.7 microtorr + 0.6 percent) in the range above 10 microtorr. When highly active gases are being used, additional errors arise because of the dependence on a calibrated mass spectrometer. Some preliminary experiments with hydrogen and with water, which will not be detailed here, suggest that a conservative estimate of the probable error in measuring the pressure of an active calibration gas is ±(1 microtorr + 1 percent).

DISCUSSION AND CONCLUDING REMARKS

This report has indicated that the probable error of the piston manometer is establishing total pressure is ±(0.5 microtorr + 0.6 percent) and that the probable error in determining net pressure of an inert calibrating gas is ±(0.7 microtorr + 0.6 percent). The accuracy in determining gage sensitivity will be poorer because the gage itself and its installation introduce additional errors. These error sources have been mentioned in the INTRODUCTION. They derive principally from variation in amount of gage pumping and from nonreproducibility of the gage characteristics because of inadequate control or definition of the gage's history and of the temperature and properties of its internal surfaces. Holanda (refs. 5 and 14) found a probable error of 3 percent in the calibration of a single gage. A similar conclusion was reached in the course of the present work with the piston manometer. Meinke and Reich (ref. 15) obtained a comparable value in their work with a commercial gage.

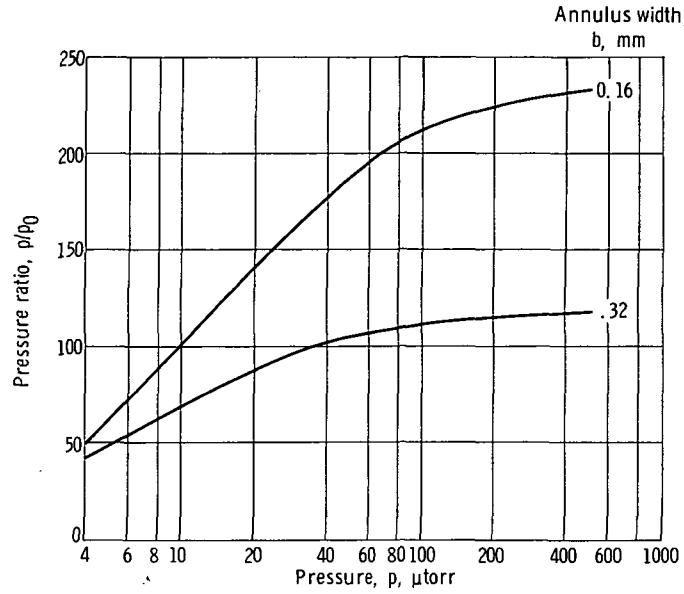

Figure 13. - Effect of annulus width on pressure ratio.

Reduction of the piston manometer's error at the low end of the pressure range, with consequent reduction of the useful low-pressure limit, requires two improvements:

1. Greater stability of dynamometer zero while retaining total-load carrying ability. Modern developments in high-vacuum microbalance techniques (refs. 16 to 23) may provide the means for accomplishing this improvement.

2. Reduction in effects of contamination due to permeation and outgassing. The number of polymeric gaskets may be reduced; in the limit, a bakeable upper plenum could be employed, but with a sacrifice of convenience. The annular gap between piston and orifice could be increased. Advantages would be shorter calibration time and a higher ratio of calibration-gas flow rate to contaminating-gas flow rate (which tends to remain constant); disadvantages would be a slight deterioration of the isobaric condition and a reduction in pressure ratio with concomitant increase in several errors. Figure 13 shows the effect on p/p_0 of doubling the gap width; the curves follow from equation (7).

Lewis Research Center,
National Aeronautics and Space Administration,
Cleveland, Ohio, September 1, 1972,
502-04.

APPENDIX A

SYMBOLS

A	effective piston area
b	annulus width
C	analogous electric capacitance, upstream plenum
C_g	analogous electric capacitance, gage
C_0	analogous electric capacitance, downstream plenum
D	orifice diameter
E_1	analogous electric potential, inlet pressure p_1
E_4	analogous electric potential, diffusion pump vapor pressure p_4
E_{20}	analogous electric potential, pumping-system blank-off pressure p_{20}
ΔF	net force on piston
G_a	vacuum conductance of annulus
I_C	electric current analogous to flow rate of contaminants in upstream plenum
$I_{C,0}$	electric current analogous to flow rate of contaminants in downstream plenum
$I_{C,4}$	electric current analogous to flow rate of contaminants at pump inlet
I_G	electric current analogous to flow rate of calibration gas
I_{GC}	$I_C + I_G$
I_g	electric current analogous to flow rate of contaminants in gage
K	Clausing factor
M	molecular weight
p	pressure in upstream plenum
p_0	pressure in downstream plenum
p_1	inlet pressure
p_2	pressure downstream of baffle
p_{20}	blank-off pressure of pumping system, downstream of baffle
R_g	analogous electric resistance, gage tubulation
R_1	analogous electric resistance, leak valve

R_2 analogous electric resistance, annulus

R_2^* analogous electric resistance, orifice

R_3 analogous electric resistance, baffle

R_4 analogous electric resistance, pump entrance

R_{34} $R_3 + R_4$

$\mathscr{R}$ universal gas constant

S gage sensitivity, collector current/pressure

s mass spectrometer sensitivity, output indication/pressure

T absolute temperature

V volume of upstream plenum

$\dot{V}_0$ volumetric pumping speed in downstream plenum

v_a arithmetic-mean molecular speed

y mass spectrometer output indication

ι^+ ion-collector current

ι^- electron-emission current

ι^-_{nom} nominal electron-emission current

τ time constant

Subscripts:

C contaminants

EIG equivalent inlet pressure of gas G[1]

G calibration gas[1]

j running index

k running index

m principal peak

R reference gas[1]

[1]Replace G or R by chemical symbol for the gas.

APPENDIX B

FABRICATION OF PISTON

The tools used for forming the piston are shown in figure 14. Ring A is used to facilitate trimming of the aluminum-foil blank. Anvils B and C are accurately alined in a

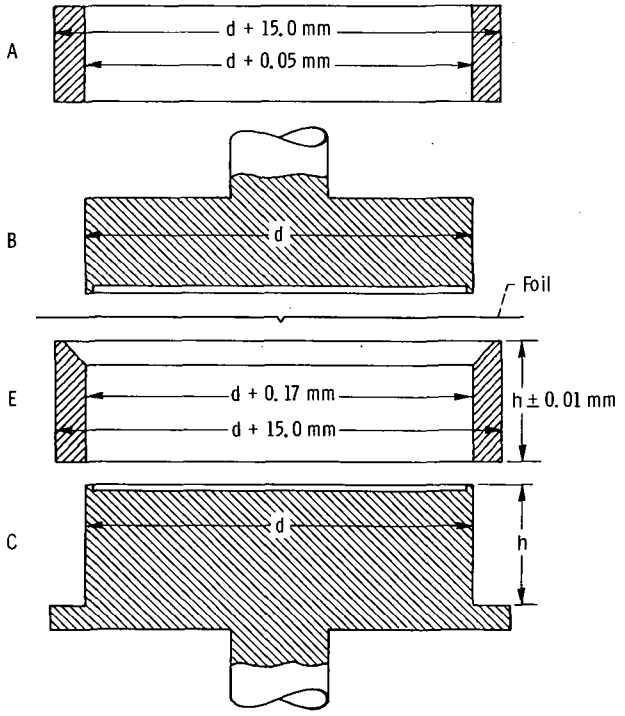

Figure 14. - Piston forming fixtures.

hydraulic press, whose axis is vertical, so that their centerlines coincide to within 0.01 millimeter; the undercuts in their faces serve to localize clamping action to the perimeter of the anvils. Ring E is used to form the vertical surfaces of the dish-shaped piston.

Steps in the forming process are as follows:

(1) Initially, with B and C mounted in the press, ring A is held above B and ring E rests on the ledge of C. All components had been thoroughly cleaned.

(2) A sheet of aluminum foil is degreased, rinsed with acetone, and dried in a hot-air stream. It is trimmed with clean scissors to a roughly octagonal shape about 16 centimeters between flats. If any natural curl remains in the sheet, the curl is removed by indenting a groove along a diameter in the direction of the curl, as illustrated in figure 14.

(3) The foil sheet is placed between the anvils, and the latter are brought together so that the foil is tightly clamped along the periphery of diameter d.

(4) Ring A is lowered over B so that A rests firmly on ring E.

(5) A clean razor blade is used to trim excess foil from the periphery of the sheet, so that there remains a circular sheet of diameter (d + 15.0 mm).

(6) Ring A is raised so that it is free of B.

(7) Ring E is raised carefully so that the protruding foil is folded upward vertically. The vertical surface becomes wrinkled, because it is folded over on itself.

(8) When ring E is raised about one half of height h, radially inward pressure is exerted progressively around the periphery, so that all wrinkles are thoroughly flattened.

(9) Ring E is raised further until it is clear of anvil B.

(10) The anvils are separated about 1 millimeter and the dish carefully slid down until it rests on anvil C.

(11) The anvil separation is continued (in 1-mm steps), the dish being made to rest on anvil C after each step, until anvil B is completely free of the dish. The stepwise process of freeing the dish from the upper anvil is necessary to prevent excessive distortion of the bottom plane of the dish.

REFERENCES

1. Warshawsky, I.: Piston Manometer as an Absolute Standard for Vacuum-Gage Calibration. J. Vacuum Sci. Tech., vol. 9, no. 1, Jan.-Feb. 1972, pp. 196-201.

2. Brombacher, W. G.: Bibliography and Index on Vacuum and Low Pressure Measurement. Mono. 35, National Bureau of Standards, Nov. 10, 1961.

3. Brombacher, W. G.: Bibliography and Index on Vacuum and Low Pressure Measurement, January 1960 to December 1965. Mono. 35, Suppl. 1, National Bureau of Standards, May 31, 1967.

4. Brombacher, W. G.: A Survey of Ionization Vacuum Gages and Their Performance Characteristics. Tech. Note 298, National Bureau of Standards, Feb. 3, 1967.

5. Holanda, Raymond: Evaluation of a Volume-Ratio System for Vacuum Gage Calibration from 10^{-8} to 10 Torr. NASA TN D-5406, 1969.

6. Ernsberger, F. W.; and Pitman, H. W.: New Absolute Manometer for Vapor Pressures in the Micron Range. Rev. Sci. Instr., vol. 26, no. 6, June 1955, pp. 584-589.

7. Reichardt, H.: Die Torsionswaage als Mikromanometer. Zeit. f. Instrumentenkunde, vol. 55, 1935, pp. 23-33.

8. Byvik, Charles E.; and Bradford, James M.: Pumping of Common Gases by Ionization Gages used in Space Simulation Facilities. AIAA/IES/ASME Space Simulation Conference. AIAA, 1966, pp. 209-214.

9. Summers, Robert L.: Empirical Observations on the Sensitivity of Hot Cathode Ionization Type Vacuum Gages. NASA TN D-5285, 1969.

10. Holanda, Raymond: Sensitivity of Hot-Cathode Ionization Vacuum Gages in Several Gases. NASA TN D-6815, 1972.

11. Whitehead, Thomas N.: The Design and Use of Instruments and Accurate Mechanism. Dover Publications, 1954.

12. Clausing, P.: Steady Flow of Highly Rarefied Gases (in Dutch). Physica, vol. 9, 1929, pp. 65-80.

13. Loeb, Leonard B.: The Kinetic Theory of Gases. Third ed., Dover Publications, 1961.

14. Holanda, Raymond: Evaluation of a Volume-Ratio Calibration System for Vacuum Gages from 10^{-6} to 10^{-3} Torr. NASA TN D-3100, 1965.

15. Meinke, C.; and Reich, G.: An Ionization Gage of Constant Sensitivity. Proceedings of the 2nd European Symposium on Vacuum. Gerhard Kienel, ed., Rudolf A. Lang Verlag, 1963, pp. 233-239.

16. Katz, Max J., ed.: Vacuum Microbalance Techniques. Vol. 1. Plenum Press, 1961.

17. Walker, Raymond F., ed.: Vacuum Microbalance Techniques. Vol. 2. Plenum Press, 1962.

18. Behrndt, Klaus H., ed.: Vacuum Microbalance Techniques. Vol. 3. Plenum Press, 1963.

19. Waters, Paul M., ed.: Vacuum Microbalance Techniques. Vol. 4. Plenum Press, 1965.

20. Behrndt, Klaus H., ed.: Vacuum Microbalance Techniques. Vol. 5. Plenum Press, 1966.

21. Czanderna, A. W., ed.: Vacuum Microbalance Techniques. Vol. 6. Plenum Press, 1967.

22. Massen, C. H.; and Van Beckum, H. T., eds.: Vacuum Microbalance Techniques. Vol. 7. Plenum Press, 1970.

23. Czanderna, A. W., ed.: Vacuum Microbalance Techniques. Vol. 8. Plenum Press, 1971.

NASA-Langley, 1972 — 14 E-6971

NATIONAL AERONAUTICS AND SPACE ADMINISTRATION
WASHINGTON, D.C. 20546

OFFICIAL BUSINESS
PENALTY FOR PRIVATE USE $300

SPECIAL FOURTH-CLASS RATE BOOK

POSTAGE AND FEES PAID
NATIONAL AERONAUTICS AND SPACE ADMINISTRATION
451

U.S.MAIL

POSTMASTER: If Undeliverable (Section 158 Postal Manual) Do Not Return

"The aeronautical and space activities of the United States shall be conducted so as to contribute . . . to the expansion of human knowledge of phenomena in the atmosphere and space. The Administration shall provide for the widest practicable and appropriate dissemination of information concerning its activities and the results thereof."

—NATIONAL AERONAUTICS AND SPACE ACT OF 1958

NASA SCIENTIFIC AND TECHNICAL PUBLICATIONS

TECHNICAL REPORTS: Scientific and technical information considered important, complete, and a lasting contribution to existing knowledge.

TECHNICAL NOTES: Information less broad in scope but nevertheless of importance as a contribution to existing knowledge.

TECHNICAL MEMORANDUMS: Information receiving limited distribution because of preliminary data, security classification, or other reasons. Also includes conference proceedings with either limited or unlimited distribution.

CONTRACTOR REPORTS: Scientific and technical information generated under a NASA contract or grant and considered an important contribution to existing knowledge.

TECHNICAL TRANSLATIONS: Information published in a foreign language considered to merit NASA distribution in English.

SPECIAL PUBLICATIONS: Information derived from or of value to NASA activities. Publications include final reports of major projects, monographs, data compilations, handbooks, sourcebooks, and special bibliographies.

TECHNOLOGY UTILIZATION PUBLICATIONS: Information on technology used by NASA that may be of particular interest in commercial and other non-aerospace applications. Publications include Tech Briefs, Technology Utilization Reports and Technology Surveys.

Details on the availability of these publications may be obtained from:

SCIENTIFIC AND TECHNICAL INFORMATION OFFICE

NATIONAL AERONAUTICS AND SPACE ADMINISTRATION

Washington, D.C. 20546